



Materials Science

An Indian Journal

Full Paper

MSAIJ, 14(3), 2016 [077-082]

Synthesis and ionic conductivity of vanadate apatite $Ba_{10}(VO_4)_6Cl_2$

Faten Nouri, Riadh Ternane*, Malika Trabelsi-Ayadi

Laboratoire d'Application de la Chimie aux Ressources et Substances Naturelles et à l'Environnement,
Université de Carthage, Faculté des Sciences de Bizerte, 7021 Zarzouna Bizerte, (TUNISIA)

E-mail : rternane@yahoo.fr

ABSTRACT

A new chlorapatite $Ba_{10}(VO_4)_6Cl_2$ has been synthesized by the solid-state reaction and characterized by X-ray diffraction, infrared absorption and Raman scattering spectroscopies.

Electrical properties of the material have been studied by the complex impedance spectroscopy. Nyquist plots show negative temperature coefficient of resistance (NTCR)-type behavior. The total conductivity of the material is thermally activated with activation energy about 0.39 eV.

© 2016 Trade Science Inc. - INDIA

KEYWORDS

Apatite;
X-ray diffraction;
Raman spectroscopy;
Complex impedance;
Electrical conductivity.

INTRODUCTION

Apatites are solid inorganic compounds, represented by the general formula $Me_{10}(XO_4)_6A_2$, Me represents a divalent cation Me can be replaced by a number of bivalent cations Ca^{2+} , Sr^{2+} , Ba^{2+} , Cd^{2+} , Pb^{2+} , but monovalent and trivalent cations such as Na^+ , K^+ and Al^{3+} can be hosted as well, XO_4 a trivalent anion is usually PO_4^{3-} , VO_4^{3-} or AsO_4^{3-} , but the possible substitutions include also SiO_4^{4-} , CO_3^{2-} and SO_4^{2-} , and A is a monovalent anion, OH, F, Cl, Br. The great variety of cationic and anionic substitutions is justified by the "open structure" of apatite. They crystallize in the hexagonal system with the space group $P6_3/m$.

The apatite-like structure is characterized by the presence of two types of tunnels permitting the location of two cationic sites labeled Me (I) and Me (II): four Me (I) are at the center of narrow tunnels (4f sites), six Me (II) around large tunnels

(6h sites), the centers of which are occupied by A⁻ anions located on the hexad axis (2a sites). The coordination number of Me (I) site is nine, whereas for Me (II), it is seven. Apatites can be used for various applications, such as catalysts^[1] and luminescent materials^[2-4] as well as in optoelectronics^[5] and biomaterials^[6]. They are also attracting considerable attention as a new class of oxide ion conductors^[7-9].

Electrical properties of the vanadate apatites have been studied, such as

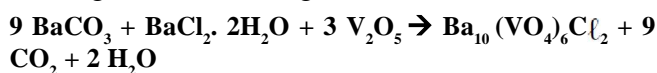
$La_{10-x}V_x(SiO_4)_6O_{3+x}$ ($0 \leq x \leq 1.5$)^[7], $Ca_{10-x}La_x(VO_4)_6O_{1+x/2}$ ^[10-11] and $Pb_8Na_2(VO_4)_6$ ^[12]. There is no study reported on the electrical properties of $Ba_{10}(VO_4)_6Cl_2$ chlorapatite.

In this study, the preparation of $Ba_{10}(VO_4)_6Cl_2$ is described. The structural characterizations have been performed using XRD, FTIR and Raman techniques. Ionic conductivity has been investigated by the complex impedance spectroscopy.

Full Paper

EXPERIMENTAL PROCEDURE

High purity $BaCO_3$ (Fluka99.9%), $BaCl_2 \cdot 2H_2O$ (Merck99.9%) and V_2O_5 (Fluka99.9%) powders have been used to prepare the apatite sample according to the following reaction:



Stoichiometric amounts of reactants have been ground and heated in covered platinum crucible at 673 K for 12 h and at 1273 K for 24 h.

Phase has been identified from the X-ray diffraction patterns using a BRUKER D8-advance diffractometer and the CuK α radiation ($\lambda = 1.5406 \text{ \AA}$). Cell parameters have been refined with the FULLPROF program. Fourier transformed infrared (FTIR) spectrum has been obtained with a BRUKER spectrometer, in the $4000\text{--}400 \text{ cm}^{-1}$ range, using the KBr pellet technique. Raman spectrum has been recorded at room temperature in the spectral range $100\text{--}1200 \text{ cm}^{-1}$ in a DILOR XY spectrometer equipped with a CCD detector and a Spectra Physics Ar laser. Conductivity measurements have been carried out from room temperature to 753 K with 20 K steps by checking the complex impedance spectroscopy with a Hewlett-Packard 4129A analyzer. The measurements have been made in the 5 Hz to

13 MHz frequency range.

RESULTS AND DISCUSSION

Characterization

X-ray powder diffraction

Figure 1 shows the X-ray patterns of the $Ba_{10}(VO_4)_6Cl_2$ sample. The patterns showed the formation of a single-phase with high degree of crystallinity of the $Ba_{10}(VO_4)_6Cl_2$ compound with a hexagonal apatite-type structure (space group $P6_3/m(176)$). It can be noticed that no secondary phase has been detected. The refined unit cell parameters are $a = 10.553 \text{ \AA}$, $c = 7.751 \text{ \AA}$ and $V = 747.549 \text{ \AA}^3$.

Vibrational infrared and raman spectra

The infrared and Raman spectra of the $Ba_{10}(VO_4)_6Cl_2$ chlorapatite are given in Figure 2 and Figure 3, respectively. The assignments of infrared (IR) and Raman bands have been performed according to the literature^[10, 12].

From Figure 2, the bands observed at 856 and 834 cm^{-1} have been assigned to the asymmetric stretching modes (ν_{as}) of VO_4 groups. However, the band appearing near 794 cm^{-1} corresponds to the symmetric stretching mode (ν_s) of VO_4 .

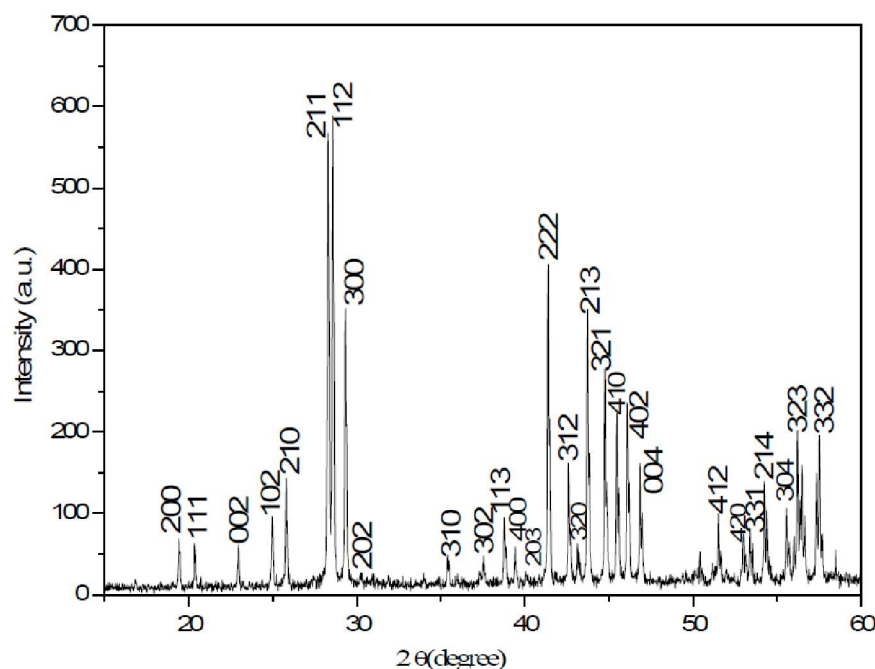


Figure 1 : X ray diffraction patterns of $Ba_{10}(VO_4)_6Cl_2$ chlorapatite

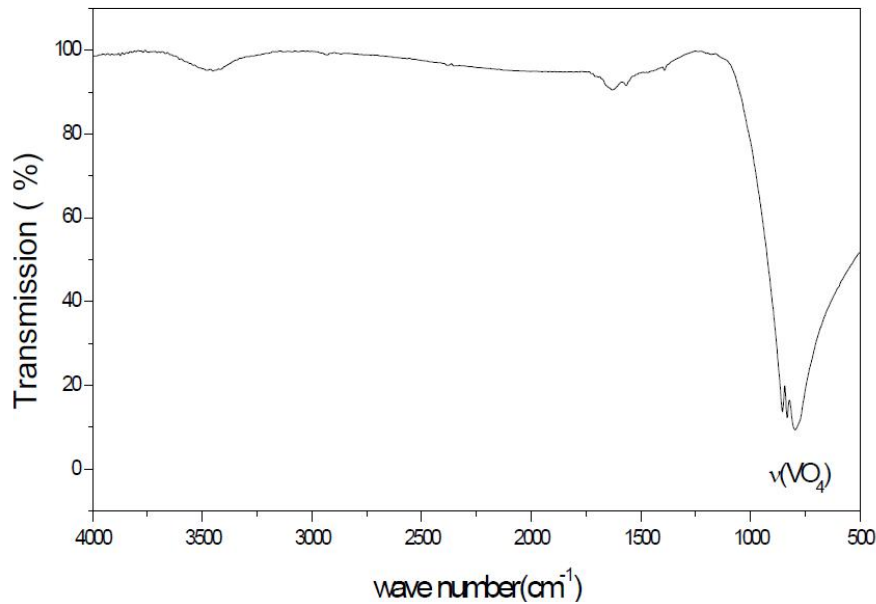


Figure 2 : IR spectrum of $\text{Ba}_{10}(\text{VO}_4)_6\text{Cl}_2$ chlorapatite

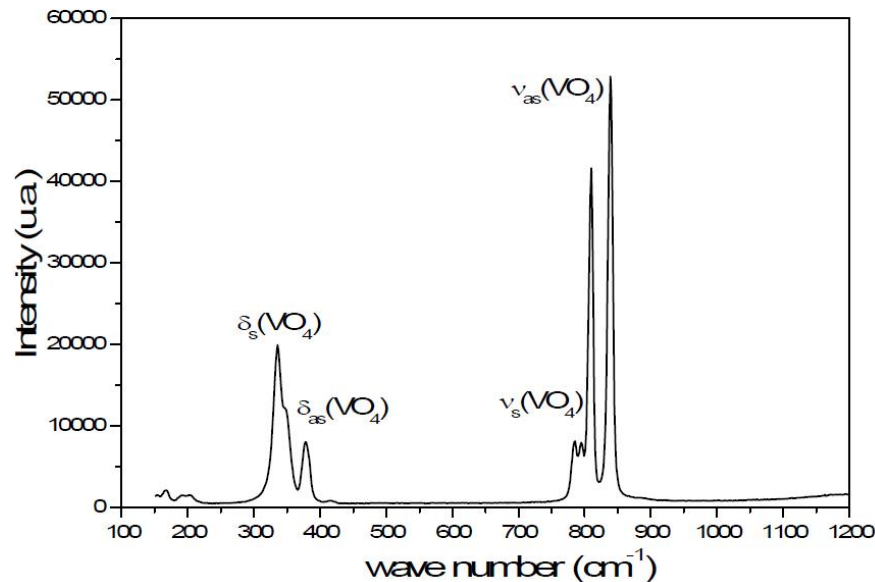


Figure 3 : Raman spectrum of $\text{Ba}_{10}(\text{VO}_4)_6\text{Cl}_2$ chlorapatite

The Raman bands at $783\text{-}794\text{ cm}^{-1}$ and $810\text{-}838\text{ cm}^{-1}$ are attributed to the symmetric (ν_s) and asymmetric (ν_{as}) stretching mode of VO_4 units, respectively. The weak bands at 377 cm^{-1} and 333 cm^{-1} can be assigned to the asymmetric δ_{as} and symmetric bending mode of VO_4 groups, respectively.

Electrical properties

Figure 4 depicts the complex impedance spectra of $\text{Ba}_{10}(\text{VO}_4)_6\text{Cl}_2$ chlorapatite at different temperatures. The effect of temperature on impedance behavior is much notable at higher temperatures. The intercept of semicircular arc with the real axis gives

an estimate of sample resistance. A very important decrease of the electrolyte resistance is observed as temperature increases indicating an activated conduction mechanism. This behavior of sample is analogous to the negative temperature coefficient of resistance (NTCR) property which is a normal behavior of semiconductor.

The total conductivity σ (TABLE 1) is calculated using the following relation:

$$\sigma = \ell/RS$$

R is the resistance obtained from impedance diagrams and S and ℓ are the area and the thickness of

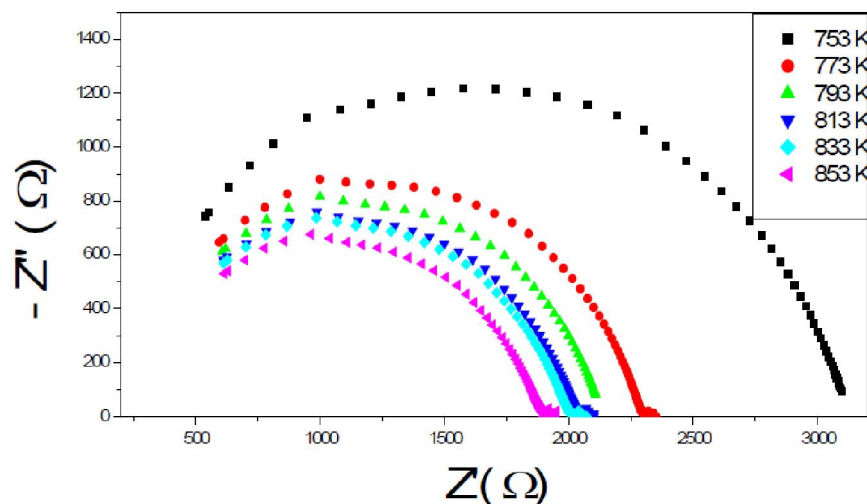


Figure 4 : Complex impedance spectra of $Ba_{10}(VO_4)_6Cl_2$ chlorapatite at different temperatures

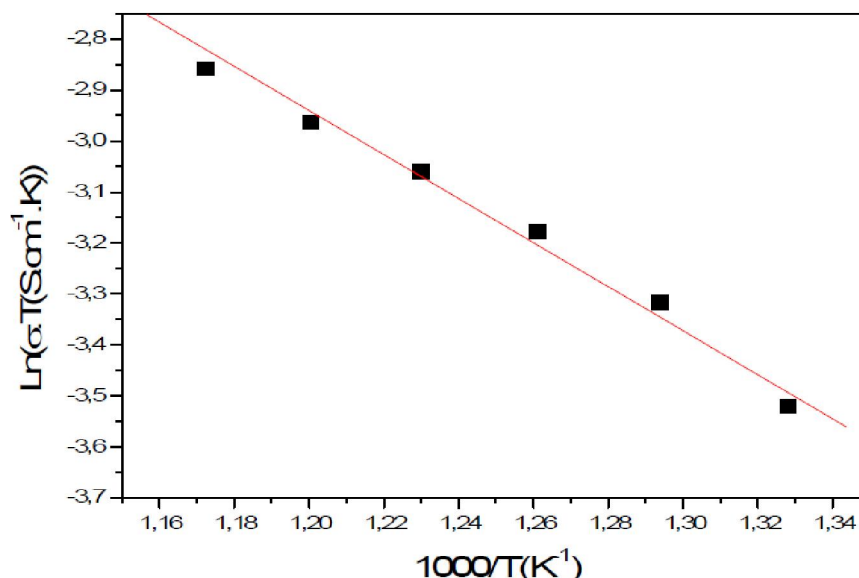


Figure 5 : Arrhenius plot $\ln(\sigma T) = f(1000/T)$ of the ionic conductivity of $Ba_{10}(VO_4)_6Cl_2$ chlorapatite

the sample, respectively.

The dependence of the total conductivity (Figure 5) of the chlorapatite electrolyte can be described by the Arrhenius equation:

$$\sigma = A/T \exp(-E_a/TK)$$

Where E_a is the activation energy, k is the Boltzmann constant and A is a pre-exponential factor. The temperature dependence of the conductivity of $Ba_{10}(VO_4)_6Cl_2$, shows a single conduction mechanism, due to absence of apparent curvature in the plot. The activation energy E_a determined from the Arrhenius plot is about 0.39 eV.

The conduction mechanism of $Ba_{10}(VO_4)_6Cl_2$ can be related to the translational hopping of chloride ions along the c axis of the unit cell from ordinary

lattice sites in interstitial sites and back again. The chloride ions must be able to move to other positions by the formation of thermally activated defects such as Schottky defects with high activation energies^[11].

TABLE 1 : Resistance and conductivity of $Ba_{10}(VO_4)_6Cl_2$ chlorapatite at different temperatures

T(K)	R(Ω)	σ (10^{-5} S.cm ⁻¹)
753	2978	3.593
773	2105	5.083
793	1971	5.428
813	1854	5.771
833	1725	6.202
853	1590	6.729

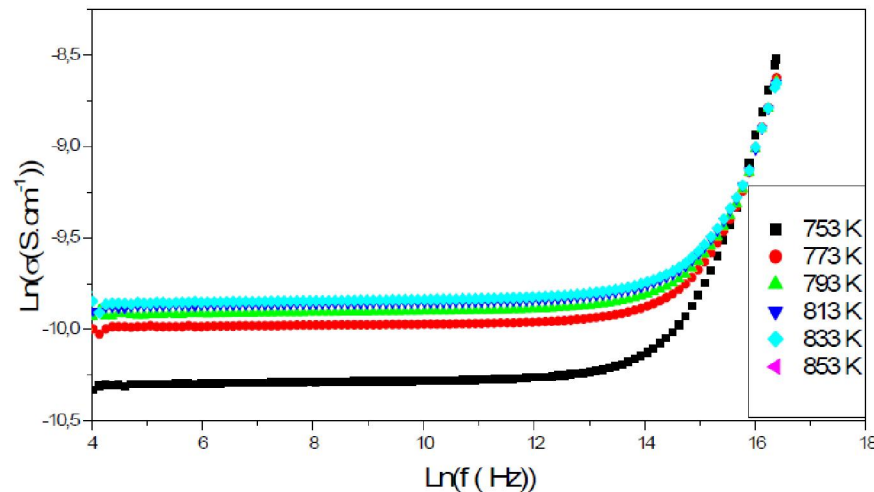


Figure 6 : Frequency dependence of the conductivity of $\text{Ba}_{10}(\text{VO}_4)_6\text{Cl}_2$ chlorapatite at different temperatures

The study of frequency dependent conductivity is a well-established method for characterizing the hopping dynamics of the charge carriers. Figure 6 shows the variation of the conductivity σ as a function of frequency at different temperatures for $\text{Ba}_{10}(\text{VO}_4)_6\text{Cl}_2$.

The frequency dependence of σ can be described by the Jonscher universal power law:

$\sigma_{ac}(\omega) = \sigma_{dc} + A(T)\omega^n$ [12,13] where σ_{ac} is an important tool for studying the ionic transport properties of materials, σ_{dc} can be obtained by extrapolating the low frequency plateau to zero frequency, ω is the angular frequency, A is the temperature dependent constant and n is an exponent, generally less than or equal to unity. As observed from the Figure 6, the behavior of conductivity σ_{ac} of $\text{Ba}_{10}(\text{VO}_4)_6\text{Cl}_2$ sample exhibits two regions in the studied range of frequency. Indeed, at low and intermediate frequencies and high temperature, a quasistatic plateau region is observed representing the dc conductivity arising from the random diffusion of the ionic charge carriers via activated hopping process [16].

The crossover frequency, ω_p is called the characteristic hopping frequency of ions and can be calculated as $\omega_p = [\sigma_{dc}/A]^{1/n}$, when $\sigma(\omega) = 2\sigma_{dc}$. Relaxation effects begin to appear at ω_p and are generally found to be thermally activated, i.e., ω_p shifts toward higher frequencies with increase in temperature.

At higher frequencies, σ_{ac} shows frequency dependence which gives rise to ac-conductivity. In this case, σ_{ac} increases roughly in a power law fashion;

$\sigma_{ac}(\omega) = A\omega^n$ and eventually becomes almost linear at even higher temperatures [17].

CONCLUSION

A single phase $\text{Ba}_{10}(\text{VO}_4)_6\text{Cl}_2$ with apatite-type structure has been synthesized successfully by solid state reaction. X-ray diffraction study shows that the sample crystallizes in the hexagonal system (space group $P6_3/m$ (176)). Infrared and Raman spectra of $\text{Ba}_{10}(\text{VO}_4)_6\text{Cl}_2$ confirm the presence of pure apatite phase without any other impurity traces, in good agreement with XRD results.

The complex impedance analysis of the sample indicated a typical negative temperature coefficient of resistance (NTCR) behavior. The temperature dependence of the electrical conductivity follows the Arrhenius law with activation energy of 0.39 eV. The frequency dependence of conductivity follows the power law.

ACKNOWLEDGEMENTS

The authors would like to thank Gerard PANCZER, Professor at the University Claude Bernard Lyon I, for his invaluable assistance in the realization of the Raman spectrum.

REFERENCES

- [1] Y. Matsumura, S. Sugiyama, H. Hayashi, J. B. Moffat; J. Solid State Chem., **114**, 138 (1971).

Full Paper

- [2] R.Ternane, M.Ferid, M.Trabelsi-Ayedi, B.Piriou, Spectrochim.Acta, **55**, 1793 (1999).
- [3] R.Ternane, G.Panczer, M.Th.Cohen-Adad, C.Goutaudier, G.Boulon, N.Kbir-Ariguib, M.Trabelsi-Ayedi; Opt.Mat., **116**, 291 (2000).
- [4] H.K.Juwhari, M.H.Kailani, B.I.Lahlouh, S.A.Abedrabbo, K.A.Saleh, W.B.White; Mater.Lett., **87**,80 (2012).
- [5] L.D.Deloach, S.A.Payne, L.K.Smith, W.L.Kway, W.F.Krupke; J.Opt.Soc.Am.B, **11**, 269 (1994).
- [6] C.Ohtsuki, T.Kokubo, T.Yamamuro; J.Non-Cryst.Solids, **143**, 84 (1992).
- [7] Y.Wenhui, S.Rongping, L.Li; Chin.J.Chem.Eng., **18**, 328 (2010).
- [8] S.Singh, B.Kumar Basu, R.Gupta; Mater.Lett., **95**,100 (2013).
- [9] D.Marrero-López, L.D.Santos-Gómez, L.León-Reina, J.Canales-Vázquez, E.R.Losilla; J.Power Sources, **245**,107 (2014).
- [10] H.Benmoussa, M.Mikou, A.Bensaoud, A.Bouhaouss, R.Morineaux; Mater.Res.Bull., **35**, 369 (2000).
- [11] A.Bouhaouss, A.Laghzizil, M.Bensaoud, G.Ferhat, J.Lorent, J.Livage; Inorg.Mater., **3**,743 (2001).
- [12] E.Chakroun-Ouadhour, R.Ternane, D.Ben Hassen-Chehimi, M.Trabelsi-Ayadi; Mater.Res.Bull., **43**, 2451 (2008).
- [13] B.Sghir, E.K.Hlil, A.Laghzizil, F.Z.Boujrhal, E.L.Cherkaoui, R.Moursli, D.Fruchart; Mater.Res.Bull., **44**, 1592 (2009).
- [14] D.P.Almond, A.R.West, R.J.Glant; Solid State Commun., **44**, 1277 (1982).
- [15] D.P.Almond, G.K.Duncan, A.R.West; Solid State Ionics, **8**,159 (1983).
- [16] J.C.Dyre; J.Appl.Phys., **64**, 2456 (1988).
- [17] K.Otto, Phys.Chem.Glasses, **7**,29(1966).